CHEMISTRY
A EUROPEAN JOURNAL

DOI: 10.1002/chem.200801942

A General Route to Construct Diverse Multifunctional Fe_3O_4/Metal Hybrid Nanostructures

Shaojun Guo,[a, b] Shaojun Dong,[a, b] and Erkang Wang*[a, b]

Abstract: We have developed a simple, efficient, economical, and general approach to construct diverse multifunctional Fe_3O_4/metal hybrid nanostructures displaying magnetization using 3-aminopropyltrimethoxysilane (APTMS) as a linker. High-density Au nanoparticles (NPs) could be supported on the surface of superparamagnetic Fe_3O_4 spheres and used as seeds to construct Au shell-coated magnetic spheres displaying near-infrared (NIR) absorption, which may make them promising in biosensor and biomedicine applications. High-density flower-like Au/Pt hybrid NPs could be supported on the surface of Fe_3O_4 spheres to construct multifunctional hybrid spheres with high catalytic activity towards the electron-transfer reaction between potassium ferricyanide and sodium thiosulfate. High-density Ag or Au/Ag core/shell NPs could also be supported on the surface of Fe_3O_4 spheres and exhibited pronounced surface-enhanced Raman scattering (SERS), which may possibly be used as an optical probe with magnetic function for application in high-sensitivity bioassays.

Keywords: gold · heterogeneous catalysis · magnetic properties · nanobiotechnology · nanostructures · Raman spectroscopy

Introduction

Magnetic nanoparticles (NPs) have been the focus of intense research because of their potential applications in magnetic fluids, catalysis, biotechnology/biomedicine, magnetic resonance imaging (MRI), magnetic recording devices, and environmental remediation.[1] With the development of nanoscience and nanotechnology, appropriate combination of different nanoscale materials may lead to the development of multifunctional nano-assembled systems that simultaneously exhibit novel optical, electronic, and magnetic properties. Synthesis and design of multicomponent hybrid nanostructures that contain two or more nanoscale components is challenging and topical owing to the multifunctional and synergistic properties induced by different functional nanoscale objects and their potential application in fields such as biomedicine and catalysis. In particular, multifunctional hybrid NPs with at least one magnetic component have recently been the subject of extensive research into combining the functionalities of magnetic NPs and semiconducting NPs (or metal nanomaterials), which endow them with interesting magnetic, semiconducting, plasmonic, and magneto-optical properties as well as potential applications in fields such as photothermal therapy, magnetic separation, and bioimaging.[2] For instance, a combination of optical and magnetic properties in a single material would enable simultaneous biolabeling/imaging and cell sorting/separation.[3] Generally, the organic-phase route has proved to be a successful methodology to obtain multifunctional nanomaterials. For instance, heterodimers with two joined NPs sharing a common interface have been synthesized by nucleation and growth of the second component on the preformed nanoparticle seeds in high-temperature organic solutions.[2,4] However, these heterostructured NPs cannot be directly utilized for biomedical applications because of their limited solubility in water and poor biocompatibility, which will greatly limit their applications. Moreover, the use of expensive organic reagents and high temperature will lead to wastage of energy. Recently, heterostructured NPs have been fabricated by integrating multiple NP components into a single nanosystem via simple aqueous-phase routes. Prominent examples include the construction of bifunctional NPs

[a] S. Guo, Prof. S. Dong, Prof. E. Wang
State Key Laboratory of Electroanalytical Chemistry
Changchun Institute of Applied Chemistry
Chinese Academy of Sciences
Changchun 130022, Jilin (China)
Fax: (+86) 431-8568-9711
E-mail: ekwang@ciac.jl.cn

[b] S. Guo, Prof. S. Dong, Prof. E. Wang
Graduate School of the Chinese Academy of Sciences
Beijing, 100039 (China)

Supporting information for this article is available on the WWW under http://dx.doi.org/10.1002/chem.200801942.

with both magnetic and optical properties by using silica[5] or polymer shells[6] as linkers, with both magnetic and catalytic properties by using silica as a linker[7] and with both magnetic and luminescent properties also with silica as linker.[8] However, complex modification and post-treatment processes are needed in the above aqueous-phase route. For instance, homogeneous silica shell coatings on the surface of one kind of NPs were usually needed, which were difficult to achieve. Kim et al.[9] reported a general synthetic procedure for multifunctional NP/silica sphere assemblies by using silica as a support, linking small Fe_3O_4 NPs by means of a very complex organic reaction, and then loading metal NPs or quantum dots (QDs) to construct bifunctional nanospheres. Although the resulting hybrid nanospheres had well-defined structure, their saturation magnetization (SM) was very low ($>4\ emu\ g^{-1}$). Therefore, it is necessary to develop an easy, rapid, inexpensive, and general method to produce diverse multifunctional hybrid NPs with high saturation magnetization (SM) to meet the requirements for potential uses in nanodevices, nanosensors, catalysis, biomedicine, and so on.

Here we report on the development of a simple, efficient, economical, and general approach to construct diverse multifunctional Fe_3O_4/metal hybrid nanostructures displaying magnetization by using 3-aminopropyltrimethoxysilane (APTMS) as a linker. Compared with the traditional linkers (e.g., silica, polymers), constructing Fe_3O_4/metal hybrid nanostructures with APTMS as a linker is simpler and more general. We found that high-density Au NPs could be supported on the surface of superparamagnetic Fe_3O_4 spheres and further used as seeds to construct Au shell-coated magnetic spheres displaying near-infrared (NIR) absorption, which could make them promising in biosensor and biomedicine applications. High-density flowerlike Au/Pt hybrid NPs could be supported on the surface of Fe_3O_4 spheres to construct multifunctional hybrid spheres with high catalytic activity towards the electron-transfer reaction between potassium ferricyanide and sodium thiosulfate. High-density Ag or Au/Ag core/shell NPs could also be supported on the surface of Fe_3O_4 spheres and exhibited pronounced surface-enhanced Raman scattering (SERS) activity, which may possibly be used as an optical probe with magnetic function for application in high-sensitivity bioassays.

Results and Discussion

The Fe_3O_4 nanospheres with the high SM were synthesized by a solvothermal method in a polyol medium according to reference [10] with some modifications. Figure 1A shows a typical transmission electron microscopy (TEM) image of Fe_3O_4 nanospheres, which have a relatively smooth surface and an average diameter of about 300 nm. After functionalization with NH_2 groups by condensation reaction of OH groups on the surface of Fe_3O_4 spheres and 3-aminopropyltrimethoxysilane (APTMS), as proved by X-ray photoelectron and FTIR spectroscopy (see below), the diameter of

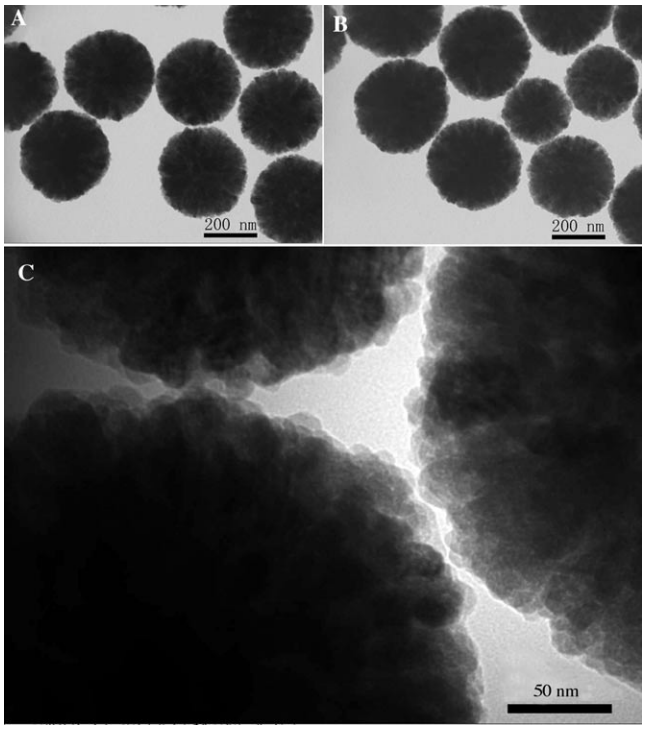

Figure 1. TEM images of Fe_3O_4 nanospheres (A) and APTMS-functionalized Fe_3O_4 nanospheres at different magnifications (B, C).

the magnetite nanospheres was not obviously changed (Figure 1B and C). These APTMS-functionalized magnetite nanospheres could adsorb diverse metal NPs with different sizes, compositions, and morphologies because of strong coordination and static interactions between the magnetite spheres and the metal NPs, which is further proof of NH_2 functionalization of the surface of the Fe_3O_4 spheres (unfunctionalized Fe_3O_4 spheres have no ability to load diverse metal NPs; data not shown). The preparation strategy for constructing diverse multifunctional Fe_3O_4/metal hybrid nanostructures is shown in Scheme 1. Figure 2A shows a low-magnification TEM image of Fe_3O_4/Au NP hybrid nanospheres. The corresponding magnified image (Figure 2B and Figure S1 in the Supporting Information) shows that 3 nm Au NPs are indeed supported on the surface of Fe_3O_4 nanospheres. Furthermore, we have demonstrated the feasibility of constructing Fe_3O_4/Au NP hybrid nanospheres using 13 nm Au NPs. As shown in Figure 2C, a great number of Fe_3O_4/Au NP hybrid nanospheres with rough surface are observed. A magnified image (Figure 2D and Figure S2 in the Supporting Information), shows that high-density Au nanoparticle (13 nm) are efficiently adsorbed on the surface of Fe_3O_4 nanospheres. Recently, several synthetic protocols for Fe_3O_4/Au hybrid NPs have been reported.[11] For instance, Bao et al.[11a] reported a multistep strategy for the synthesis of bifunctional Au/Fe_3O_4 hybrid NPs that are formed by chemical bond linkage. In comparison, our method is simpler. More importantly, our strategy easily allows more Au NPs to be adsorbed to give high-density of Au NPs supported on Fe_3O_4 hybrid NPs.

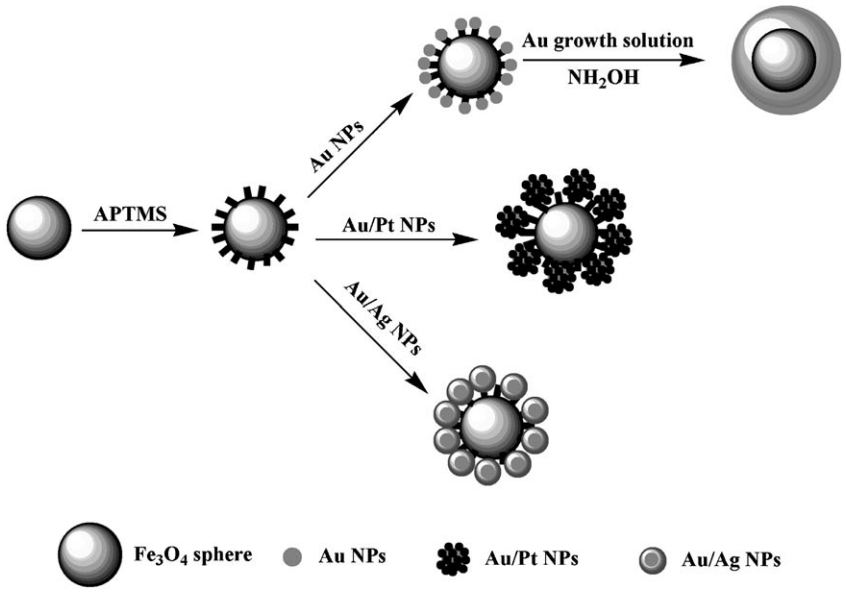

Scheme 1. Fabrication of diverse multifunctional Fe_3O_4/metal hybrid nanostructures.

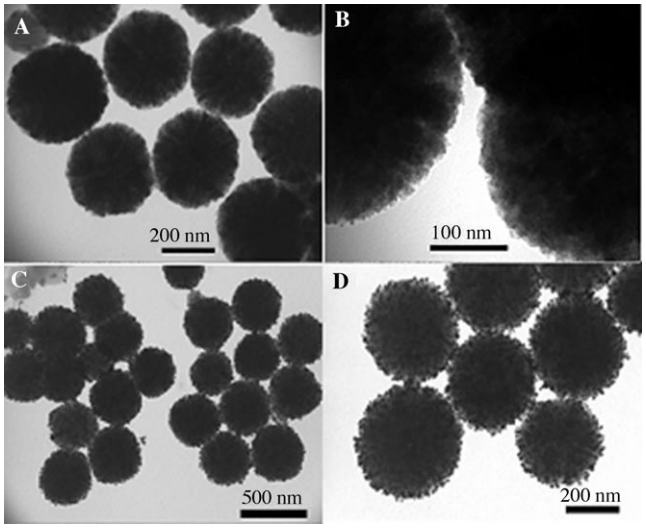

Figure 2. TEM images of Au NPs (ca.3 nm) supported on Fe_3O_4 hybrid nanospheres (A, B) at different magnifications and Au NPs (ca. 13 nm) supported Fe_3O_4 hybrid nanospheres at different magnifications (C, D).

The functionalized Fe_3O_4 nanospheres can also adsorb other metal NPs. For instance, high-density flowerlike Au/Pt hybrid NPs could also be adsorbed on the surface of Fe_3O_4 nanospheres, as shown in Figure 3. Low-magnification images (Figure 3A–C) show that a large number of hybrid spheres with very rough surface were obtained. Magnified images (Figure 3D and inset; Figure S3 in the Supporting Information) indicate that Au/Pt hybrid NPs supported on surface of Fe_3O_4 nanospheres have a flowerlike structure. We expected that these Au/Pt hybrid NPs supported hybrid Fe_3O_4 nanospheres could be used as recyclable catalysts with high catalytic activity (see below). In addition, these functionalized Fe_3O_4 nanospheres could also adsorb silver NPs (ca. 3 nm, Figure 4A) and Au/Ag core/shell NPs (ca. 40 nm, Figure 4B). The fact that a high density of NPs could again be supported on the surface of Fe_3O_4 nanospheres to construct multifunctional hybrid nanostructures indicates that our method is a general one for constructing different hybrid nanostructures based on magnetic nanospheres. We also found that it was hard to construct diverse multifunctional nanostructures using non-functionalized Fe_3O_4 spheres as substrates (data not shown). This indicates that the NH_2 groups on the surface of the Fe_3O_4 spheres play an important role in constructing diverse

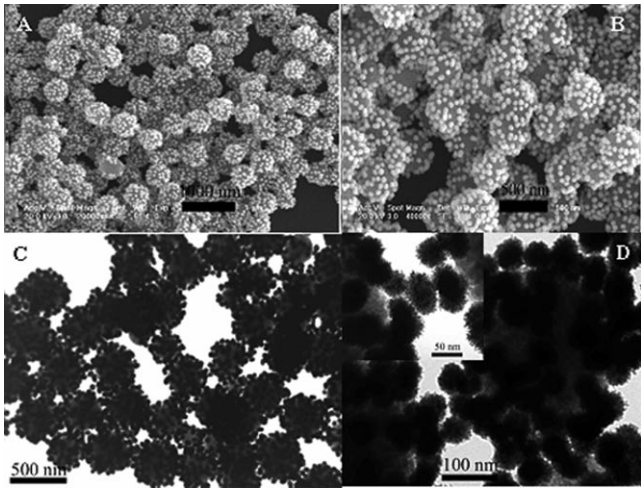

Figure 3. SEM (A, B) and TEM (C, D) images of the flowerlike Au/Pt hybrid NPs supported Fe_3O_4 hybrid nanospheres

multifunctional nanostructures, probably due to strong coordinative interactions between the NH_2 groups and metal nanostructures and/or static interactions between NH_2-functionalized Fe_3O_4 and negatively charged metal nanostructures.

The Fe_3O_4/Au hybrid nanostructures were further characterized by energy-dispersive X-ray (EDX) and X-ray photoelectron spectroscopy (XPS). The EDX spectrum (Figure 5) shows peaks corresponding to Au, Fe, and N, confirming the presence of Au NPs and NH_2 groups on the surface of the Fe_3O_4 nanospheres. The XPS patterns (Figure 6A–C) of the Fe_3O_4/Au hybrid nanostructure show significant Fe 2p signal corresponding to the binding energy of Fe (Figure 6A), significant Au 4f signal corresponding to the binding energy of metallic Au (Figure 6B), and an N 1s signal characteristic of

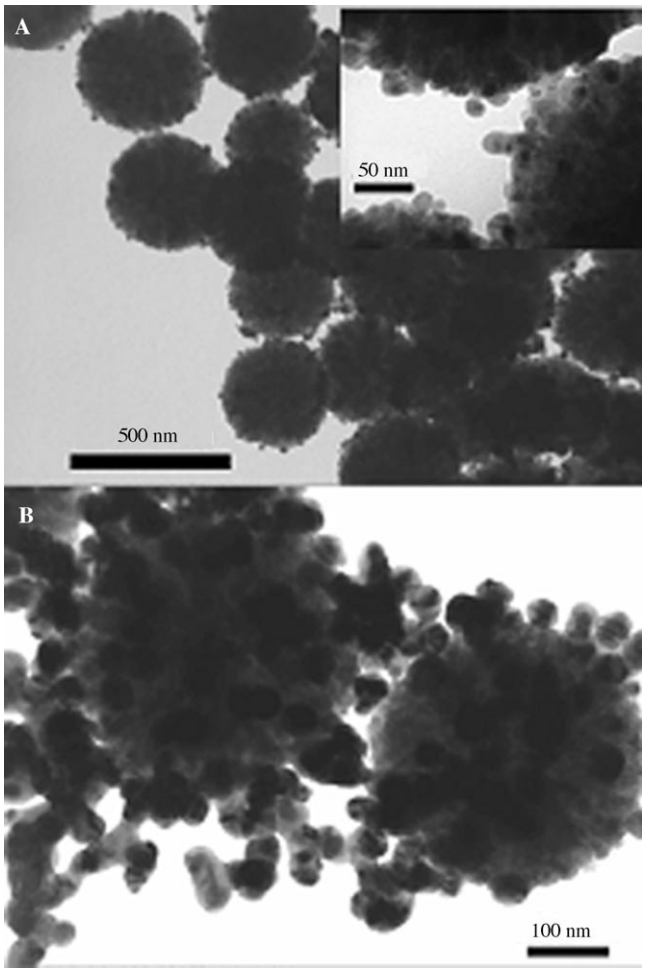

Figure 4. A) TEM images of Ag NPs (ca. 3 nm) and B) Au/Ag core/shell NPs supported on Fe_3O_4 hybrid nanospheres.

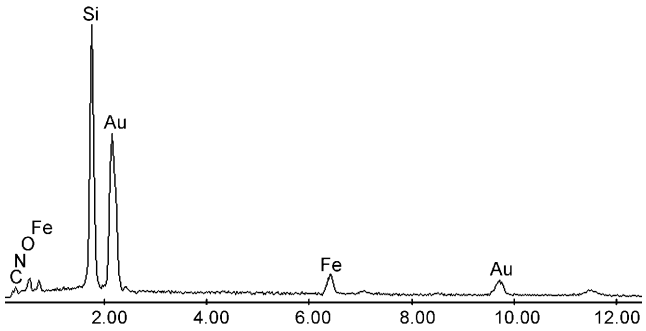

Figure 5. EDX image of Fe_3O_4 hybrid nanospheres coated with an Au shell.

NH_2 (Figure 6C), which support the above conclusion that the surface of the Fe_3O_4 spheres have been functionalized with NH_2 groups. The FTIR spectrum of APTMS-functionalized Fe_3O_4 NPs is shown in Figure 6D. The strong IR band at 575 cm^{-1} is characteristic of Fe–O vibrations,[12] while the bands around 876, 1630, and 3434 cm^{-1} can be ascribed to NH_2 groups located on the surface of Fe_3O_4 NPs. Two other peaks at 2930 and 1448 cm^{-1} are associated with the C–H stretching and deformation vibrations of APTMS, respectively. Zeta potential measurements of surface charge were further used to monitor the functionalization process of Fe_3O_4 nanospheres. The ζ value measured for nonfunctionalized Fe_3O_4 was about −8.44 mV, ascribed to surface hydroxyl groups. On functionalization with APTMS, however, the ζ value increased to about +8.43 mV. Thus, FTIR and ζ potential data further prove that APTMS effectively functionalized the surface of the Fe_3O_4 nanospheres.

Photothermal therapy in the NIR region is very important in the field of biomedicine, because blood and soft tissue are relatively transparent in this region, so that collateral damage to surrounding healthy tissue is minimized.[13] Over the past few years, many research efforts have been devoted to developing novel Au nanostructures to achieve surface plasma resonance (SPR) in the NIR region for biomedical applications such as photothermal therapy. To date, Au nanocages,[13,14] nanorods,[15,16] nanorings[17] and silica-supported Au nanoshells[18] have served as very efficient photothermal therapeutic agents. Compared with the above NIR absorption materials, bifunctional Au-coated magnetic nanospheres have the advantage that their movement can be controlled with an external magnetic field so that they can be immobilized close to the target tissue for more efficient therapy. To this end, we have developed a rapid strategy for obtaining Au/Fe_3O_4 shell/core hybrid nanospheres which exhibit NIR absorption by using magnetic nanospheres decorated with Au NPs as seeds in the presence of a growth solution. Figure 7A and B show typical SEM images of Au/Fe_3O_4 shell/core hybrid nanospheres obtained by adding 0.3 mL of $HAuCl_4$ (1%) to the growth solution in the presence of Fe_3O_4/Au NPs (ca.3 nm). The magnified image (Figure 7B) shows that a discontinuous Au shell was formed on the surface of the Fe_3O_4 nanospheres. The corresponding TEM images (Figure 7C and D) further support the above statement. Thus, 0.3 mL of $HAuCl_4$ solution was insufficient for obtaining well-defined Au-coated Fe_3O_4 nanospheres. On continuously increasing the amount of $HAuCl_4$ (1%) to 1 mL, many well-defined Au-coated Fe_3O_4 hybrid nanospheres were obtained, as shown in the SEM images of Figure 8A and B. The TEM images of the as-made Au-coated Fe_3O_4 hybrid nanospheres show well-separated individual nanoparticle structures with relatively smooth Au shells (Figure 8C and D). On increasing the amount of $HAuCl_4$ to 2 mL, Fe_3O_4 hybrid nanosphere cores with thicker Au shells but poor structure (some hybrid particles seem to be aggregated) were obtained (Figure 8E and F), that is, an excess of $HAuCl_4$ (2 mL) is not effective for obtaining Au/Fe_3O_4 shell/core hybrid nanospheres.

Ultraviolet/visible/near-IR absorption spectroscopy was carried out to confirm that the as-prepared Au-coated Fe_3O_4 hybrid nanospheres display the NIR absorption of the Au nanoshells (Figure 9B). The absorption spectrum of Au NPs supported on magnetite nanospheres shows no absorption in the NIR region (Figure 9B, curve a). The absorption located at around 600 nm can be ascribed to the Fe_3O_4 sphere

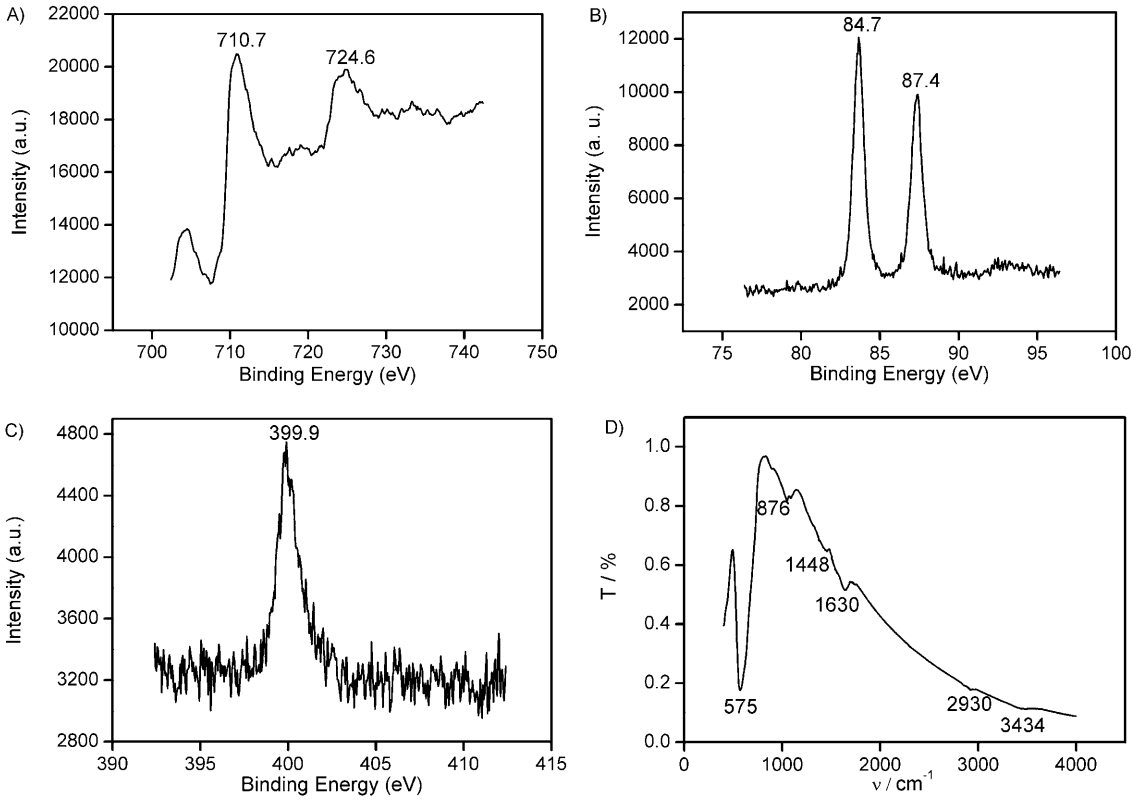

Figure 6. XPS patterns of Fe_3O_4 hybrid nanospheres coated with Au NPs (ca. 3 nm). A) Fe 2p; B) Au 4f; C) N 1s. D) FTIR spectrum of APTMS-functionalized Fe_3O_4 nanospheres.

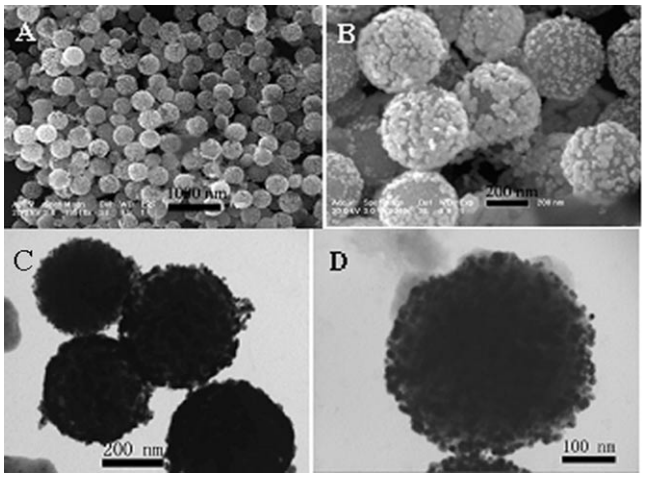

Figure 7. SEM (A, B) and TEM (C, D) images of Fe_3O_4 hybrid nanospheres coated with discontinuous Au shells (prepared by adding 0.3 mL of 1% $HAuCl_4$) at different magnifications.

itself.[6] After reductive deposition of Au onto the existing surface of the Au seeds to form discontinuous Au nanoshells by adding 0.3 mL of 1% $HAuCl_4$ solution, absorption in the NIR range started to appear (Figure 9B, curve b). On increasing the amount of $HAuCl_4$ to 1 mL (Figure 9B, curve c) and 2 mL (Figure 9B, curve d), NIR absorptions were clearly observed, in accordance with previous report.[6] The

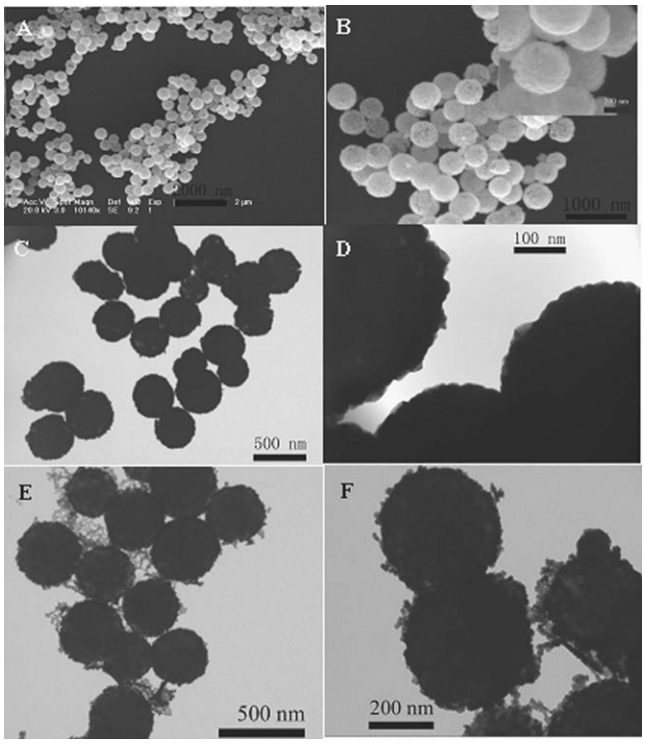

Figure 8. SEM (A, B) and TEM (C, D) images of Fe_3O_4 hybrid nanospheres coated with Au shells (prepared by adding 1 mL of 1% $HAuCl_4$) at different magnifications. TEM images (E, F) of Fe_3O_4 hybrid nanospheres coated with Au shells (adding 2 mL of 1% $HAuCl_4$) at different magnifications.

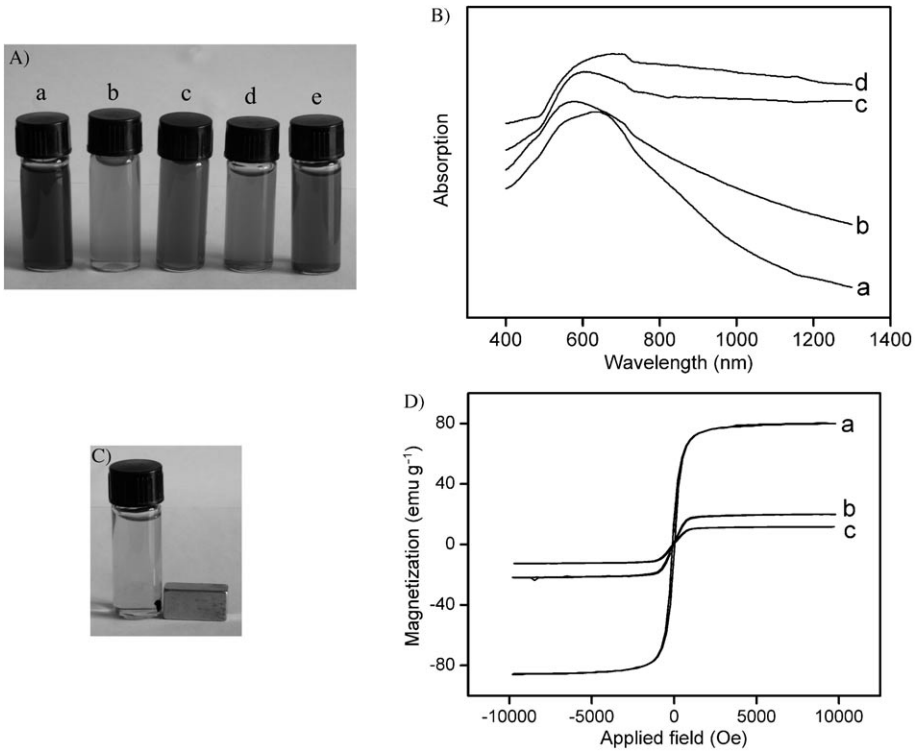

Figure 9. Photographs (A) of the NP solutions in sunlight. a) Fe_3O_4 nanospheres. b) Au NPs (ca.3 nm) supported on Fe_3O_4 hybrid nanospheres. c) Fe_3O_4 hybrid nanospheres coated with discontinuous Au shells (prepared by adding 0.3 mL of 1% $HAuCl_4$). d) Fe_3O_4 hybrid nanospheres coated with Au shells (prepared by adding 1 mL of 1% $HAuCl_4$). e) Fe_3O_4 hybrid nanospheres coated with Au shells (prepared by adding 2 mL of 1% $HAuCl_4$). NIR absorption spectra (B). Curve a: Au NPs (ca. 3 nm) supported on Fe_3O_4 hybrid nanospheres; curve b: Fe_3O_4 hybrid nanospheres coated with discontinuous Au shells (prepared by adding 0.3 mL of 1% $HAuCl_4$); curve c: Fe_3O_4 hybrid nanospheres coated with Au shells (prepared by adding 1 mL of 1% $HAuCl_4$); curve d: Fe_3O_4 hybrid nanospheres coated with Au shells (prepared by adding 2 mL of 1% $HAuCl_4$). Photograph (C) of Fe_3O_4 hybrid nanospheres coated with Au shells (prepared by adding 2 mL of 1% $HAuCl_4$) after magnetic separation by an external magnetic field. Magnetization curves (D) of Fe_3O_4 spheres (curve a), Fe_3O_4 hybrid nanospheres coated with Au shells (prepared by adding 1 mL of 1% $HAuCl_4$, curve b), and Fe_3O_4 hybrid nanospheres coated with Au shells (prepared by adding 2 mL of 1% $HAuCl_4$, curve c).

change in the absorption spectra is also reflected in the colors of the colloidal suspensions of the hybrid NPs. Figure 9A shows how the colors of Fe_3O_4 (a), Au seeds (3 nm) supported on Fe_3O_4 (b), and Fe_3O_4 nanospheres with different Au shells (c–e) change from brown to dark blue with formation of the Au nanoshells. Magnetization curves (Figure 9D) were measured on powder samples of Fe_3O_4 nanospheres (curve a) and Au-coated Fe_3O_4 hybrid nanospheres (curves b and c for samples obtained by adding 1 and 2 mL of 1% $HAuCl_4$ solution, respectively) at room temperature. They exhibit negligible coercivity and remanence, and their SM values are 80.5, 20.6, and 12.5 emu g^{-1}, respectively. The decrease in SM can be explained by taking into account the diamagnetic contribution of the Au shell surrounding the magnetic cores (the magnetic cores amount to about 25 wt% of the magnetic Au spheres).[8] However, the SM values of the present materials are much larger than those reported by Salgueiriño-Maceira et al.[5,8] and Kim et al.[9] The strong magnetization of the hybrid NPs (addition of 1 mL of 1% $HAuCl_4$) was also revealed by the fact that they were easily attracted by an external magnetic field over a short time (less than 40 s, Figure 9C). This strategy is also a general one and can be easily extended to prepare other Au/Fe_3O_4 shell/core hybrid nanospheres of different sizes (by just changing the size of the Fe_3O_4 spheres) and with well-defined NIR absorption. These core-shell hybrid NPs with novel optical and magnetic properties may have potential applications in photothermal therapy, magnetic resonance imaging, and targeted-delivery applications.

Recyclable, bifunctional magnetic nanospheres with high catalytic activity have received considerable interest because of their easy removal from reaction mixtures. For instance, Yi et al. reported that silica-coated magnetic NPs could be used as a catalyst supports for constructing hybrid nanospheres containing Pd NPs. The resulting Fe_2O_3/SiO_2/Pd nanocomposite catalyst is easily recycled by magnetic separation while keeping high catalytic activity towards hydrogenation of nitrobenzene.[19] However, high-density flowerlike Au/Pt hybrid NPs supported Fe_3O_4 nanospheres (Figure 3) prepared via a simple method have not been studied as recyclable catalysts. The present hybrid nanospheres possibly have advantages such as high catalytic activity (it has been shown that the flowerlike Au/Pt hybrid nanostructures used here[20] have a large catalytically active area, and Fe_3O_4 nanospheres can be used as a 3D supports for further increasing the effective surface-to-volume ratio of Au/Pt hybrid NPs) and ease of recycling by magnetic separation. The electron-transfer reaction between $[Fe(CN)_6]^{3-}$ and $S_2O_3^{2-}$ was employed as an example to demonstrate the catalytic activity of the bifunctional hybrid nanospheres.[21] The decline of the $[Fe(CN)_6]^{3-}$ peaks with and without bifunctional hybrid nanospheres as a function of time was monitored by the absorption at about 420 nm. The absorption was monitored every 10 min for 60 min and the kinetics experiments were carried out at 25 °C. Without bifunctional hybrid nanospheres, a small spectral decline was observed (Figure 10B). For bifunctional hybrid nanospheres (Figure 10A), the significant change in the band peak intensity in the absorption spectrum of $[Fe(CN)_6]^{3-}$ indicated good

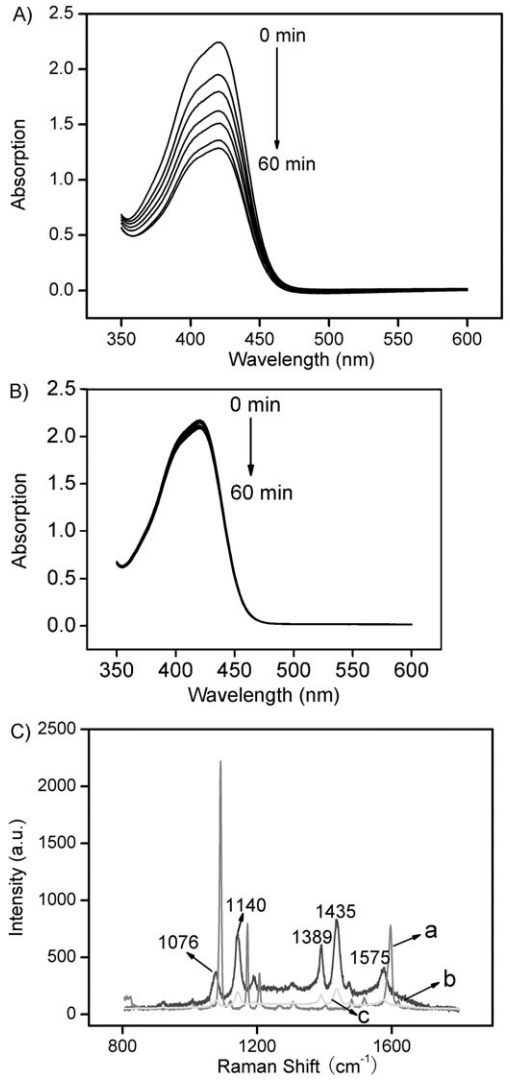

Figure 10. A) UV/Vis/NIR spectral changes of $[Fe(CN)_6]^{3-}$ during its reaction with $S_2O_3^{2-}$ at 25 °C in the presence of flowerlike Au/Pt hybrid NPs supported on Fe_3O_4 nanospheres. B) Reaction in the absence of catalyst. C) SERS spectrum of 4-ATP adsorbed on Au/Ag core/shell NPs (curve c), Au/Ag core/shell NPs supported on Fe_3O_4 hybrid nanospheres (curve b), and Raman spectrum of solid 4-ATP (curve a).

catalytic activity of the hybrid nanospheres. These bifunctional hybrid nanospheres could be easily recycled by means of an external magnetic field (data not shown) and still keep their high activity after recycling five times. (Hybrid NPs are stable even under the conditions of sonication; data not shown.) Most importantly, this strategy can be extended to immobilize other Pt- and Pd-based nanomaterials with different sizes and morphologies on the surface of Fe_3O_4 nanospheres to obtain recyclable high-activity catalysts for different catalytic reactions.

Raman-active NPs, as a class of emerging labels, have been attracting considerable attention due to their applications in high-sensitivity bioassays. Traditional methods are based on direct attachment of both the Raman reporter and biomolecule to the NP probe.[22] However, individual spherical Au NPs, which produced relatively weak Raman signals for small organic compounds as labels, were employed. According to theoretical calculations, a molecule at the junction between aggregated NPs can produce Raman scattering intensity several orders of magnitude higher than a molecule on the surface of a single spherical NP.[23] To the best of our knowledge, Au/Ag core/shell NP aggregates, which generally exhibit higher SERS activity than Au nanomaterial aggregates, supported on magnetic nanospheres have not been extensively pursed for use as Raman tags as they are difficult to prepare. Thus, it would be interesting to explore whether the as-prepared hybrid magnetic nanospheres containing Au/Ag core/shell NP aggregates could be used for fabricating substrates for intense SERS. Figure 10C (curve b) depicts the SERS spectrum of 4-aminothiophenol (4-ATP) molecules absorbed on the surface of hybrid nanospheres. Compared with the normal Raman spectrum of solid 4-ATP (Figure 10C, curve a), noticeable shifts in frequency can be observed from the SERS spectra on hybrid nanosphere-modified substrates, that is, the thiol group of 4-ATP directly contacts with the silver surface.[24] Two sets of bands were observed in the SERS spectra of 4-ATP in the assembled film. One set, located at 1076 cm^{-1}, is assigned to the a_1 vibration modes, and the other, located at 1140, 1389, 1435, and 1575 cm^{-1}, to the b_2 vibration modes.[25] As reported by Osawa et al.,[26] enhancement of b_2 modes is attributed to the chemical mechanism, most likely due to charge transfer (CT) from the adsorbate to the metal. Furthermore, a hybrid-nanosphere-modified glass substrate exhibited excellent SERS activity when a low concentration of 4-ATP was employed (comparable intensity to the Raman peak of solid 4-ATP). If 4-ATP is adsorbed at high concentration on the surface of hybrid nanospheres, it is expected that better SERS activity will be obtained. Furthermore, the substrate modified with hybrid nanospheres exhibited higher SERS activity than Au/Ag core/shell NPs (curve c). Thus, hybrid-nanosphere-modified SERS substrates will potentially find applications in high-sensitivity bioassays based on magnetic separation, such as detecting DNA and proteins.

Conclusion

We have explored a simple, efficient, and general route to obtain diverse multifunctional hybrid nanospheres based on Fe_3O_4 nanospheres. This method has some clear advantages including simplicity, speed, and good reproducibility. Our study is significant for the following reasons: 1) High-density Au NPs could be supported on the surface of superparamagnetic Fe_3O_4 spheres and further used as seeds to construct Au-shell-coated magnetic spheres displaying NIR absorption, which are possibly promising in biosensor and biomedicine applications. 2) High-density flowerlike Au/Pt hybrid NPs could be supported on the surface of Fe_3O_4 spheres to construct multifunctional hybrid spheres with high catalytic activity towards the electron-transfer reaction between potassium ferricyanide and sodium thiosulfate. 3) High-density

Ag or Au/Ag core/shell NPs supported on the surface of Fe_3O_4 nanospheres exhibit excellent SERS activity, which will possibly be used as optical probe with magnetic function for application in magnetic separation based bioassays. 4) The present strategy can also be extended to prepare other hybrid nanomaterials based on large or small Fe_3O_4 magnetic nanospheres. Further research on several other important applications such as biosensors, nanodevices, and electrocatalysis are underway.

Experimental Section

Materials: Trisodium citrate, vitamin C, $FeCl_3 \cdot 6H_2O$, $HAuCl_4 \cdot 4H_2O$, $H_2PtCl_6 \cdot 6H_2O$, $AgNO_3$, $NH_2OH \cdot HCl$, CH_3COONa, $K_3[Fe(CN)_6]$, $Na_2S_2O_3$, poly(*N*-vinyl-2-pyrrolidone) (PVP·K30), ethylene glycol (EG), and ethanol were purchased from Shanghai Chemical Factory (Shanghai, China) and used as received without further purification. 3-Aminopropyltrimethoxysilane (APTMS), 4-aminothiophenol (4-ATP), and $NaBH_4$ were obtained from Aldrich. Water used throughout all experiments was purified with the Millipore system.

Apparatus: An XL30 ESEM scanning electron microscope (SEM) was used to determine the morphology and composition of products. Transmission electron microscopy (TEM) measurements were made on a HITACHI H-8100 EM with an accelerating voltage of 200 kV. The sample for TEM characterization was prepared by placing a drop of prepared solution on a carbon-coated copper grid and dried at room temperature. X-ray photoelectron spectroscopy (XPS) was performed on an ESCALAB-MKII spectrometer (VG Co., United Kingdom) with $Al_{K\alpha}$ X-ray radiation as the X-ray source for excitation. The sample for XPS characterization was dropped onto a glass slide. UV/Vis/NIR spectra were collected on a CARY 500 Scan UV/Vis/NIR spectrophotometer. SERS spectra were obtained on a J-Y T64000 Raman spectrometer using an Olympus microscope and a 50× long working distance objective to focus the laser beam onto a spot of about 1 μm^2. Zeta potentials were measured by dynamic light scattering (Zetasizer 3000, Malvern Instruments, France). Infrared spectra were collected in transmission mode on a Nicolet 520 FTIR spectrometer.

Synthesis and functionalization of magnetic Fe_3O_4 nanopheres: a) The Fe_3O_4 nanospheres with high saturation magnetization were synthesized by a solvothermal method in polyol medium according to reference [10] with some modifications (using PVP as a protecting agent). b) For APTMS-functionalized Fe_3O_4 spheres, Fe_3O_4 nanospheres (20 mg) were added to ethanol (30 mL), followed by the addition of water (2 mL). Then, ammonium hydroxide (25%; 2 mL) and APTMS (200 μL) were added to the above solution. The resulting solution was sonicated for about 8 h. After four-step separation by means of an external magnetic field, the resulting product was dissolved in water (10 mL).

Synthesis of NPs with different size, morphology, and composition: a) 13 nm Au NPs were synthesized according to reference [27] Thus, a 1 mM $HAuCl_4$ solution (100 mL) was brought to reflux while stirring and then 38.8 mM trisodium citrate solution (10 mL) was added quickly, which resulted in a color change of the solution from pale yellow to deep red. The solution was then heated to reflux for an additional 15 min. The concentration of Au NPs was about 1 mM provided that $HAuCl_4$ was completely reduced. b) The Au NPs with a diameter of about 3 nm were synthesized according to the literature.[28] c) In a typical synthesis of Ag NPs with a diameter of about 3 nm, a 0.2 M aqueous solution of $AgNO_3$ (0.5 mL) was rapidly added to water (100 mL) with vigorous stirring, followed by addition of 1% aqueous citrate solution (10 mL). A quick color change was observed on addition of excess $NaBH_4$ (0.1 M, 5 mL). d) The flowerlike Au/Pt hybrid NPs were synthesized by the following procedure.[20] First, 1 wt% $HAuCl_4$ aqueous solution (1 mL) was added to water (100 mL) and heated to boiling while stirring. Then 1 wt% sodium citrate (1.5 mL) was quickly introduced into the above solution. After heating for several minutes, appearance of a gold-red solution indicated formation of Au NPs (ca. 25 nm). Then 0.2 M vitamin C (excess; 1 mL) was subsequently added to the boiling solution of Au nanoparticles, followed by 1 wt% H_2PtCl_6 (2.5 mL). In this process, heat treatment clearly accelerated the kinetics of reduction of the Pt salt by vitamin C on the colloidal Au surface. After heating for 20 min, flowerlike Au/Pt hybrid NPs were obtained. e) The Au/Ag core/shell NPs were synthesized by a procedure similar to method d with minor modifications. First, 1 wt% $HAuCl_4$ aqueous solution (1 mL) was added to water (100 mL) and heated to boiling while stirring. Then sodium citrate solution (1 wt%; 1.5 mL) was quickly introduced to the above solution. After heating for several minutes, the solution was allowed to cool to room temperature. Then 0.2 M vitamin C (excess; 1.5 mL) was subsequently added to the solution of Au NPs at room temperature, followed by the addition of 0.2 M $AgNO_3$ (0.375 mL). After the mixture had been stirred for 20 min, the Au/Ag core/shell NPs were obtained.

Constructing Fe_3O_4/metal hybrid nanostructures: a) The Fe_3O_4/metal NP hybrid nanostructures were prepared by mixing an aqueous solution of APTMS-functionalized Fe_3O_4 nanospheres (1 mL) with 10–20 mL of a solution of Au, Ag, flowerlike Au/Pt, or Au/Ag core/shell NPs (excess). The resulting products were collected by means of an external magnet and dissolved in 1 mL of water. b) For synthesis of Fe_3O_4/Au shell hybrid nanospheres displaying magnetization and NIR absorption, 1 mL of the above solution was added to water (10 mL), followed by the addition of 1% citrate solution (2 mL) and 0.1 M NH_2OH solution (1 mL). Then, 1% $HAuCl_4$ (1 mL; for 0.3 or 2 mL $HAuCl_4$, the volume of 0.1 M NH_2OH should be decreased or increased, accordingly) was added dropwise to the above solution with shaking.

SERS measurements: For SERS studies, an aqueous solution of hybrid nanospheres with Au/Ag core/shell NPs or Au/Ag core/shell NPs supported on Fe_3O_4 (20 μL) was added dropwise onto a glass substrate and dried under ambient conditions, and then a 2.0×10^{-4} M ethanolic solution of 4-ATP (20 μL) was added dropwise onto the resulting nanostructure film and allowed to dry. After washing the substrate with ethanol and drying by N_2, SERS spectra were recorded under ambient conditions.

Catalytic properties of flowerlike Au/Pt hybrid NPs supported on Fe_3O_4 hybrid nanospheres: For the electron-transfer reaction between potassium ferricyanide and sodium thiosulfate, 0.1 M potassium ferricyanide (0.1 mL) and hybrid nanosphere solution (0.5 mL) were added to water (4.3 mL), and the solution was kept at 25 °C. The catalytic reaction was initiated by adding 1 M sodium thiosulfate solution (0.1 mL). The reaction was monitored by in situ UV/Vis/NIR absorption spectroscopy.

Acknowledgement

This work was supported by the National Science Foundation of China (Nos. 20575063, 2057506, and 2067507) and the 973 Project 2007CB714500.

[1] A. Lu, E. L. Salabas, F. Schüth, *Angew. Chem.* **2007**, *119*, 1242–1266; *Angew. Chem. Int. Ed.* **2007**, *46*, 1222–1244.
[2] H. Zeng, S. Sun, *Adv. Funct. Mater.* **2008**, *18*, 391–400.
[3] F. X. Redl, K. S. Cho, C. B. Murray, S. O'Brien, *Nature* **2003**, *423*, 968–971.
[4] for example: a) S. T. Selvan, P. K. Patra, C. Y. Ang, J. Y. Ying, *Angew. Chem.* **2007**, *119*, 2500–2504; *Angew. Chem. Int. Ed.* **2007**, *46*, 2448–2452; b) K. W. Kwon, M. Shim, *J. Am. Chem. Soc.* **2005**, *127*, 10269–10275; c) J. Choi, Y. Jun, S. Yeon, H. C. Kim, J. Shin, J. Cheon, *J. Am. Chem. Soc.* **2006**, *128*, 15982–15983; d) Z. Xu, Y. Hou, S. Sun, *J. Am. Chem. Soc.* **2007**, *129*, 8698–8699; e) H. Gu, R. Zheng, X. Zhang, B. Xu, *J. Am. Chem. Soc.* **2004**, *126*, 5664–5665; f) T. Pellegrino, A. Fiore, E. Carlino, C. Giannini, P. D. Cozzoli, G. Ciccarella, M. Respaud, L. Palmirotta, R. Cingolani, L. Manna, *J. Am. Chem. Soc.* **2006**, *128*, 6690–6698; g) H. Yu, M. Chen, P. M. Rice, S. X. Wang, R. L. White, S. Sun, *Nano Lett.* **2005**, *5*, 379–382; h) Y. Li, Q. Zhang, A. V. Nurmikko, S. Sun, *Nano Lett.* **2005**, *5*,

1689–1692; i) W. Shi, H. Zeng, Y. Sahoo, T. Y. Ohulchanskyy, Y. Ding, Z. L. Wang, M. Swihart, P. N. Prasad, *Nano Lett.* **2006**, *6*, 875–881.
[5] a) V. Salgueiriño-Maceira, M. A. Correa-Duarte, M. Farle, A. Lopez-Quintela, K. Sieradzki, R. Diaz, *Chem. Mater.* **2006**, *18*, 2701–2706; b) M. A. Correa-Duarte, V. Salgueiriño-Maceira, B. Rodríguez-González, L. M. Liz-Marzán, A. Kosiorek, W. Kandulski, M. Giersig, *Adv. Mater.* **2005**, *17*, 2014–2018.
[6] L. Wang, J. Bai, Y. Li, Y. Huang, *Angew. Chem.* **2008**, *120*, 2473–2476; *Angew. Chem. Int. Ed.* **2008**, *47*, 2439–2442.
[7] J. Ge, T. Huynh, Y. Hu, Y. Yin, *Nano. Lett.* **2008**, *8*, 931–934.
[8] V. Salgueiriño-Maceira, M. A. Correa-Duarte, M. Spasova, L. M. Liz-Marzán, M. Farle, *Adv. Funct. Mater.* **2006**, *16*, 509–514.
[9] J. Kim, J. E. Lee, J. Lee, Y. Jang, S.-W. Kim, K. An, J. H. Yu, T. Hyeon, *Angew. Chem.* **2006**, *118*, 4907–4911; *Angew. Chem. Int. Ed.* **2006**, *45*, 4789–4793.
[10] H. Deng, X. L. Li, Q. Peng, X. Wang, J. P. Chen, Y. D. Li, *Angew. Chem.* **2005**, *117*, 2842–2845; *Angew. Chem. Int. Ed.* **2005**, *44*, 2782–2785.
[11] a) J. Bao, W. Chen, T. Liu, Y. Zhu, P. Jin, L. Wang, J. Liu, Y. Wei, Y. Li, *ACS Nano* **2007**, *1*, 293–298; b) S. I. Stoeva, F. Huo, J. Lee, C. A. Mirkin, *J. Am. Chem. Soc.* **2005**, *127*, 15362–15363; c) J. L. Lyon, D. A. Fleming, M. B. Stone, P. Schiffer, M. E. Williams, *Nano Lett.* **2004**, *4*, 719–723.
[12] L. Wang, J. Bao, L. Wang, F. Zhang, Y. Li, *Chem. Eur. J.* **2006**, *12*, 6341–6347.
[13] J. Chen, D. Wang, J. Xi, L. Au, A. Siekkinen, A. Warsen, Z. Li, H. Zhang, Y. Xia, X. Li, *Nano Lett.* **2007**, *7*, 1318–1322.
[14] J. Y. Chen, B. Wiley, Z. Y. Li, D. Campbell, F. Saeki, H. Cang, L. Au, J. Lee, X. D. Li, Y. N. Xia, *Adv. Mater.* **2005**, *17*, 2255–2261.
[15] C. C. Chen, Y. P. Lin, C. W. Wang, H. C. Tzeng, C. H. Wu, Y. C. Chen, C. P. Chen, L. C. Chen, Y. C. Wu, *J. Am. Chem. Soc.* **2006**, *128*, 3709–3715.
[16] X. H. Huang, I. H. El-Sayed, W. Qian, M. A. El-Sayed, *J. Am. Chem. Soc.* **2006**, *128*, 2115–2120.
[17] E. M. Larsson, J. Alegret, M. Kall, D. S. Sutherland, *Nano Lett.* **2007**, *7*, 1256–1263.
[18] L. R. Hirsch, R. J. Stafford, J. A. Bankson, S. R. Sershen, B. Rivera, R. E. Price, J. D. Hazle, N. J. Halas, J. L. West, *Proc. Natl. Acad. Sci. USA* **2003**, *100*, 13549 13554.
[19] D. K. Yi, S. S. Lee, J. Y. Ying, *Chem. Mater.* **2006**, *18*, 2459–2461.
[20] S. Guo, L. Wang, S. Dong, E. Wang, *J. Phys. Chem. C* **2008**, *112*, 13510–13515.
[21] a) M. A. Mahmoud, C. E. Tabor, M. A. El-Sayed, Y. Ding, Z. L. Wang, *J. Am. Chem. Soc.* **2008**, *130*, 4590–4591; b) W. Yang, Y. Ma, J. Tang, X. Yang, *Colloids Surf.A* **2007**, *302*, 628–633.
[22] a) Y. C. Cao, R. C. Jin, C. A. Mirkin, *Science* **2002**, *297*, 1536–1540; b) Y. C. Cao, R. C. Jin, J. M. Nam, C. S. Thaxton, C. A. Mirkin, *J. Am. Chem. Soc.* **2003**, *125*, 14676–14677.
[23] C. Wang, Y. Chen, T. Wang, Z. Ma, Z. Su, *Adv. Funct. Mater.* **2008**, *18*, 355–361.
[24] G. Wei, L. Wang, Z. Liu, Y. Song, L. Sun, Y. Yang, Z. Li, *J. Phys. Chem. B* **2005**, *109*, 23941–23947.
[25] J. W. Zheng, X. W. Li, Y. Ji, R. A. Gu, T. H. Lu, *J. Phys. Chem. B* **2002**, *106*, 1019–1023.
[26] M. Osawa, N. Matsuda, K. Yoshi, I. Uchida, *J. Phys. Chem.* **1994**, *98*, 12702–12707.
[27] a) S. Guo, S. Dong, E. Wang, *Small* **2008**, *4*, 1133–1138; b) S. Guo, L. Wang, S. Dong, E. Wang, *J. Phys. Chem. C* **2008**, *112*, 13510–13515; c) S. Guo, J. Li, E. Wang, *Chem. Asian J.* **2008**, *3*, 1544–1548.
[28] a) K. C. Grabar, K. J. Allison, B. E. Baker, R. M. Bright, K. R. Brown, R. G. Freeman, A. P. Fox, C. D. Keating, M. D. Musick, M. J. Natan, *Langmuir* **1996**, *12*, 2353–2361; b) S. Guo, Y. Fang, J. Zhai, S. Dong, E. Wang, *Chem. Asian J.* **2008**, *3*, 1156–1162; c) S. Guo, S. Dong, E. Wang, *J. Phys. Chem. C* **2008**, *112*, 2389–2393.

Received: September 19, 2008
Published online: January 13, 2009

